RESEARCH ARTICLE

Nutritional Endoderm in a Direct Developing Frog: A Potential Parallel to the Evolution of the Amniote Egg

Daniel R. Buchholz,[1†] Srikanth Singamsetty,[2] Uma Karadge,[2] Sean Williamson,[2] Carrie E. Langer,[2] and Richard P. Elinson[2*]

The egg of the direct-developing frog, *Eleutherodactylus coqui*, has 20× the volume as that of the model amphibian, *Xenopus laevis*. Increased egg size led to the origin of nutritional endoderm, a novel cell type that provides nutrition but does not differentiate into digestive tract tissues. As the *E. coqui* endoderm develops, a distinct boundary exists between differentiating intestinal cells and large yolky cells, which persists even when yolk platelets are depleted. The yolky cells do not become tissues of the digestive tract and are lost, as shown by histology and lineage tracing. *EcSox17*, an endodermal transcriptional factor, did not distinguish these two cell types, however. When cleavage of the yolky cells was inhibited, embryogenesis continued, indicating that some degree of incomplete cleavage can be tolerated. The presence of cellularized nutritional endoderm in *E. coqui* may parallel changes that occurred in the evolution of the amniote egg 360 million years ago. *Developmental Dynamics 236:1259–1272, 2007.* © 2007 Wiley-Liss, Inc.

Key words: *Eleutherodactylus coqui*; direct development; endoderm; yolk; *Sox17*; lineage tracing; amniote egg; amniote evolution

Accepted 14 March 2007

INTRODUCTION

A key innovation in the evolution of the terrestrial vertebrates was the amniote egg. The amniote egg generates not only the embryo, but also a set of extraembryonic membranes that support development on land. In addition to these membranes, the amniote egg is characterized by a large amount of yolk and by meroblastic cleavage, which does not divide the yolk into cells. In contrast to the large yolky egg of turtles, snakes, lizards, and birds, extant amphibians have eggs that are usually 1–5 mm in diameter, and all have complete or holoblastic cleavage. The amphibian mode is considered basal for terrestrial vertebrates, because egg size, cleavage, and gastrulation in amphibians is similar to lungfish and sturgeon, among others (Elinson, 1989; Collazo et al., 1994). This situation raises the question as to how a meroblastic cleaving egg evolved from a holoblastic cleaving one.

This evolution occurred approximately 360 million years ago, so it is unlikely that traces of these changes in soft, embryonic tissues will be found in the fossil record. A source of information for possible scenarios is to examine amphibians with large yolky eggs to see how increased yolk affects early development. One such amphibian, available for experimental analysis, is the Puerto Rican tree frog, *Eleutherodactylus coqui*. Its egg is 3.5 mm in diameter, 20× the volume of the egg of the frog model *Xenopus laevis*.

The large egg size in *E. coqui* is associated with differences in molecular organization of early embryonic patterning as compared with *X. laevis*. The RNA for *EcVegT*, the orthologue

[1]Section on Molecular Morphogenesis, LGRD, NICHD, NIH, Bethesda, Maryland
[2]Department of Biological Sciences, Duquesne University, Pittsburgh, Pennsylvania
Grant sponsor: the National Science Foundation; Grant number: IBN-0080028; Grant number: IOB-0343403.
[†]Dr. Buchholz's present address is Department of Biological Sciences, University of Cincinnati, Cincinnati, OH 45221.
***Correspondence to: Richard P. Elinson, Department of Biological Sciences, Duquesne University, Pittsburgh, PA 15282. E-mail: elinson@duq.edu**

DOI 10.1002/dvdy.21153
Published online 18 April 2007 in Wiley InterScience (www.interscience.wiley.com).

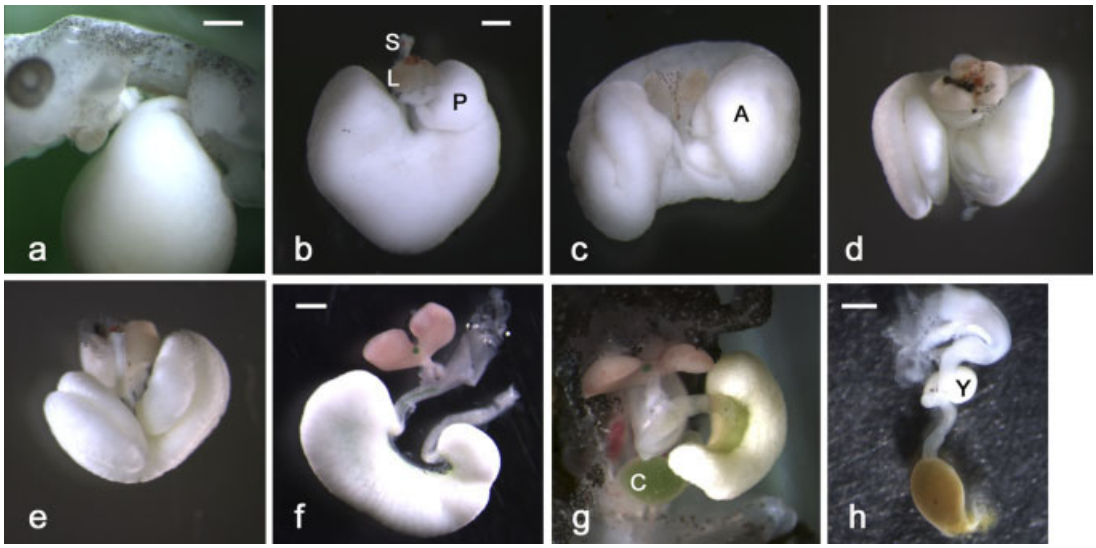

Fig. 1.

of the *X. laevis* endo–mesodermal determinant, is concentrated in the animal cytoplasm of the oocyte, rather than localized to the vegetal cortex (Beckham et al., 2003). Mesoderm-inducing activity is restricted to marginal surface in the *E. coqui* early gastrula and is absent from the deeper, yolky cells and the vegetal pole (Ninomiya et al., 2001). These differences led us to propose a different fate map for *E. coqui*, in which ectodermal and mesodermal tissues are displaced above the equator, near the animal pole, compared with *X. laevis* (Ninomiya et al., 2001; Elinson and Beckham, 2002). The prospective endoderm is greatly enlarged.

In the investigation reported here, we examined the development of the endoderm in *E. coqui*. We present evidence that most of the yolk-rich region of the early embryo serves only a nutritional role and does not contribute to differentiated tissues or organs of the digestive system. This condition may parallel the one that occurred in the evolution of the amniote egg.

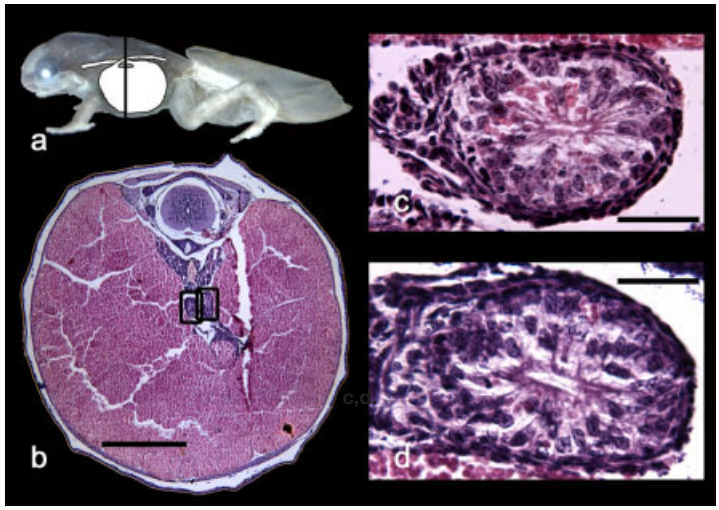

Fig. 2.

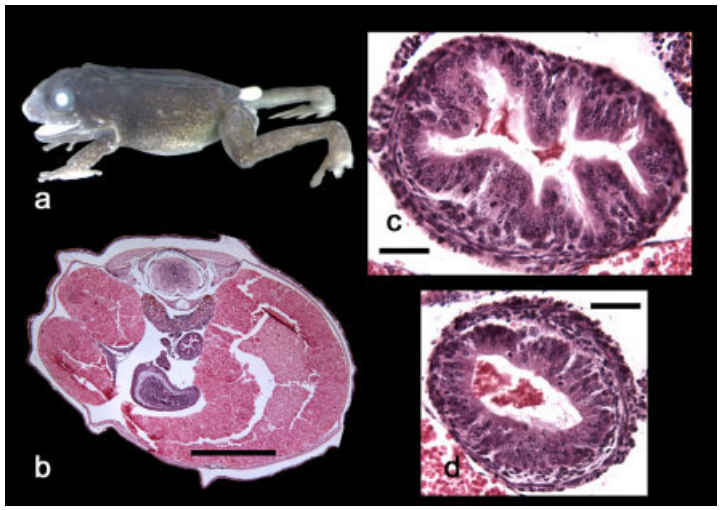

Fig. 3.

RESULTS

Gross Morphology of Intestine Development

The egg of *E. coqui* has approximately 20× the volume of the egg of *X. laevis*. The increased volume is due to yolk, required to support the nonfeeding embryo to a free-living frog. Cleavage

and gastrulation are similar to amphibians with smaller eggs, but the embryo develops directly to a frog without passing through a tadpole stage (see Fig. 10 for selected stages). The frog hatches from its jelly capsule approximately 3 weeks after fertilization. It still has a large amount of yolk, which enables it to grow for 1–2 weeks before eating.

As the gut initially forms, the large mass of yolky cells, the yolky endoderm, is connected to the mouth and the anus by thin tubes. This simple arrangement persists until TS 9. At this stage, the embryo looks quite frog-like with big eyes, limbs, and digits, atop the yolk (Fig. 10c). At TS 9, the yolky endoderm turns by 90 degrees, so the original anterior–posterior axis becomes the right–left axis (Fig. 1a). Consequently, the anterior tube bends to the right to enter the yolky endoderm, and the posterior tube exits from left of the midline. Beginning at TS 10, the anterior tube becomes translucent, and differentiation into stomach, liver, and lungs is apparent (Fig. 1b).

Over the next few days, represented by stages TS 10–13, the yolky endoderm becomes longer, with greater elongation on the ventral side than on the dorsal side. To accommodate this elongation, the anterior and posterior ends of the yolky endoderm are folded dorsally and in toward the midline. Due to these folds, there is an anterior and a posterior lobe, with a more pronounced fold separating the posterior lobe from the rest of the yolky endoderm (Fig. 1c). The yolky endoderm is like a thick sash or belt. Its outer surface is pressed against the ventral and lateral sides of the coelom. It is folded in on itself dorsally, so that from a dorsal aspect, there is an anterior lobe and a posterior lobe with the stomach, liver, and heart in between (Fig. 1c).

To achieve the final morphology, the gut has bent and folded (Fig. 1d,e). The folding is topologically complicated, because the elongation of the gut is far less on the side attached to the dorsal mesentery. The entry of the anterior tube into the yolky endoderm and the exit of the posterior tube remain relatively close together, while the opposite side of the yolky endoderm elongates more. The folding then is more like the folding of a fan, rather than the complete coils present in the gut of the developing *X. laevis* embryo (Chalmers and Slack, 1998). This complex coiling exists in most tadpoles, as they are herbivorous, and little if any trace of the tadpole-type gut is present in the nonfeeding *E. coqui* embryo.

As the amount of yolk decreases after hatching (TS 15), the anterior and posterior lobes diminish and disappear, and the internal luminal surface becomes smooth. Consequently, the gut of the hatched froglet has an unusual appearance because of the presence of large yolky cells in the future intestinal region (Fig. 1f,g). The dorsal surface of the yolky endoderm, attached to the mesentery, is translucent like the differentiated tissues of the stomach anteriorly and the hindgut posteriorly, but it joins laterally to a large mass of yolky cells (Fig. 1g). The presence of this dorsal translucent tissue is highlighted by the large amount of green bile pigments, released from the gall bladder. As yolk is used, the yolk mass shrinks, and the gut becomes a continuous tube of digestive tissues (Fig. 1h). The cloaca often is swollen with wastes.

The morphology of the developing gut suggests that the large yolky cells are distinct from the cells forming the rest of the intestine. We consider this possibility further by histology, lineage tracing, and expression of an endodermal marker.

Prehatching Intestinal Histology

Before hatching, the anterior and posterior tubular structures and the yolky endoderm as described above are distinct in histology (Fig. 2). The

Fig. 1. Gross morphology of digestive tract development. **a:** TS 9 embryo. The ventral skin and body wall of this TS 9 embryo were removed to see the orientation of the gut. The posterior tube exits from the left side of the yolk-rich region and runs posteriorly to the anus. This left exit is caused by a 90-degree rotation of the yolk-rich region. **b:** TS 10 gut. This isolated TS 10 gut, viewed from ventral side, has liver (L) and a stomach (S), which enters the yolk-rich region to the embryo's right (left in this ventral view). There is a fold to produce a posterior lobe (P) in the yolk-rich region on the embryo's left, from which the posterior tube exits. **c:** TS 12 gut. This isolated TS 12 gut viewed from the dorsal side shows the fold to produce a posterior lobe on the embryo's left (left in this dorsal view as well) from which the posterior tube exits. The liver and stomach are in the top center, and the anterior tube from the stomach enters an anterior lobe (A), which has folded less than the posterior one. **d,e:** Early TS 15 gut viewed from dorsal (d) and posterior (e) aspects. The posterior lobe is deeply folded, and the developing organs sit between the posterior and anterior lobes of the yolk-rich region. **f:** Post-TS 15 gut. This isolated gut was dissected from a froglet and extended to reveal the relationship between the different areas. The two pink liver lobes and the green gall bladder are connected to the anterior tube at the base of the stomach. The anterior tube enters the yolk-rich region, and the posterior tube exits from it. **g:** Post-TS 15 gut. The froglet was dissected and the yolk-rich region was displaced to the frog's left to reveal the relationships. The gall bladder has released a large amount of green bile pigments. These highlight the translucent tissue on the dorsal surface of the yolk-rich region, which is connected to the anterior and posterior tubes. The bile accumulates in the cloaca (C). **h:** Gut from a late prefeeding froglet. A small amount of yolk (Y) remains in the intestine of this isolated gut. The cloaca is filled with brown bile pigments and yolk debris. Scale bars = 0.5 mm. b–e and g are the same scale.

Fig. 2. Histology of the prehatching digestive tract. **a:** TS 14 embryo, removed from the egg capsule, with a diagram of the intestine superimposed. The vertical line indicates the plane of the cross-section in the next panel. **b:** A cross-section at level shown in (a) indicates a large amount of yolk taking up the majority of the peritoneal volume. Boxes indicate areas photographed at higher magnification in the next panels. **c:** Cross-section of the anterior tube reveals undifferentiated epithelium and a small lumen. **d:** Cross-section of the posterior tube shows similar histology as in (c). Note yolk platelets (magenta) in anterior and posterior tubes. Scale bar = 1 mm in b, 10 μm in c,d.

Fig. 3. Intestinal remodeling after hatching. **a:** TS 15 froglet with tail nearly gone. **b:** Cross-section through the whole body shows less yolk and more intestinal loops than seen in Figure 2b. **c:** The anterior tube has multiply folded epithelium and an absence of yolk in the epithelial cells. **d:** The posterior tube also lacks yolk in the epithelial cells but has not undergone epithelial remodeling. In both anterior and posterior tubes, muscle (outer ring of cells) has differentiated from the connective tissue (cells between muscle and epithelium). Scale bar = 1 mm in b, 10 μm in c,d.

anterior and posterior tubes are similar in that there are two cell layers, an outer layer one to two cells thick of undifferentiated connective tissue with very little cytoplasm and an inner columnar epithelial layer facing the small lumen (Fig. 2c,d). The columnar layer seems to be a single layer of cells with unaligned nuclei, but it is possible that there are multiple layers where not all cells are in contact with the basal lamina, presumed to be present between the connective tissue and epithelial cells. Yolk is still present in the epithelial cells at this stage (Fig. 2c,d). Mitotic figures are often seen.

The yolky endoderm fills the majority of the abdominal cavity (Fig. 2b). Nuclei are widely dispersed throughout this tissue, and cell boundaries are often not readily observable in histological sections. This appearance reflects the difficulty in fixation of this yolk-rich tissue, as in some preparations, individual cells are clearly visualized (e.g., Fig. 11). The cellular nature of the yolky endoderm was confirmed by direct observation of dissected, living embryos at TS 3 (neurula) and TS 6 (gill circulation). In addition, when placed into 100% Ca^{2+}-free Steinberg's solution with 0.5 mM ethyleneglycoltetraacetic acid (EGTA), the yolky endoderm dissociated into a large pile of cells. The yolky endoderm is surrounded by the mesentery, a squamous layer of connective tissue, distinct from the undifferentiated connective tissue around the anterior and posterior tubes.

Intestinal Remodeling

Histological remodeling of the intestine begins when most of the yolk is still present (Fig. 3a,b). Between TS 14 and TS 15, the anterior tube changes from a simple tube to the more complex structure of the adult (Fig. 3c). The epithelium becomes multiply folded, and the presumptive muscle around the outside and connective tissue cells in between the muscle and epithelium become distinct. In the posterior tube, muscle and connective tissue are visible, but the epithelial in-folding seen in the anterior tube has not yet occurred (Fig. 3d).

Beginning at TS 15, the process of replacing the yolky endoderm with intestinal epithelium begins, and this replacement can be considered a second phase of intestinal remodeling. Intestinal epithelium first develops between the anterior and posterior tubes on the dorsal surface of the yolky endoderm tube, starting from both ends (Fig. 4a). Simultaneously, there is a ventrally directed expansion of the epithelium along the walls of the yolky endoderm tube, so that the surface area of epithelium expands and yolky endoderm decreases (Fig. 4b–d). The epithelial expansion along dorsal surface connects from both ends before the ventral expansion is 50% complete. Thus, the intestinal epithelium proper gradually replaces the yolky endoderm. Simultaneous with this second phase of histological remodeling, the number of yolk platelets in the yolky endoderm cells decreases. However, yolk platelets actually disappear before many of the yolky endoderm cells are replaced. These changes leave two distinct kinds of cells facing the lumen: the intestinal epithelium and the now depleted yolky endoderm cells, with only a few cells having a few yolk platelets (Fig. 4e,f).

Fate of the Yolky Endoderm Cells

The histology described above raised the question of whether the yolky endoderm cells contribute to the epithelium proper. Before TS 15, yolk is present in all intestinal endoderm cells, that is, the yolky endoderm as well as the epithelial cells of the anterior and posterior tubes. An exclusive histological distinction develops between yolky endoderm and adult intestinal regions, as the cells of the anterior and posterior tubes gradually lose yolk. By the time intestinal remodeling is complete and yolky endoderm replacement has begun at TS 15, no yolk platelets exist in any cell except the yolky endoderm. The presence of intracellular yolk platelets is a unique identifier of yolky endoderm. In addition, even when depleted of yolk and reduced in size near border regions, the shape of nuclei and staining characteristics of the yolky endoderm are distinct from the epithelium proper (Fig. 4e,f).

The histological distinctiveness of the yolky endoderm suggests that it might not become part of the epithelium. To address whether the depleted yolky endoderm cells die by apoptosis, terminal deoxynucleotidyl transferase–mediated dUTP nick end-labeling (TUNEL) assay was carried out at different stages of intestine remodeling. This assay failed to detect cell death, even when yolk was completely depleted (data not shown), suggesting apoptotic cells are not common enough to detect or the yolky endoderm cells die by some other mechanism. Evidence for an alternate death mechanism comes from serial sections of intestine, when most of the yolky endoderm is depleted. At this time, it is common to see cells apparently being sloughed into the lumen (Fig. 5). The two examples shown are taken from a large number of such observations seen exclusively in the depleted yolky endoderm regions. In addition, close examination of the sloughed cells indicated that in every case, there were multiple nuclei inside each cell, suggesting that each yolky endoderm cell is multinucleate. Further evidence of sloughing is that at this stage, the posterior intestinal lumen is filled with nuclei, an occurrence not seen at other stages.

Fate Mapping

Histological examination suggests that the yolky endoderm does not become differentiated intestinal tissue. To test this suggestion further, large vegetal cells of morulae, with approximately 40–60 cells (Fig. 6), were injected with the lineage tracer fluorescein dextran amine (FDA), and their fate was followed. Embryos were raised to different stages, when their digestive tract was dissected out and examined for FDA fluorescence. Of the 50 animals, 13 were prehatching (TS 9–TS 15), 13 within the first week posthatching, 15 within the second week posthatching, 8 within the third week, and 1 at 27 days posthatching.

Injection of FDA into vegetal cells labeled only the large, yolky cells of the endoderm and not differentiated gut tissues in 43 of 50 cases. In six cases, there were specks of FDA in the liver as well as labeled yolky endoderm. The remaining froglet was

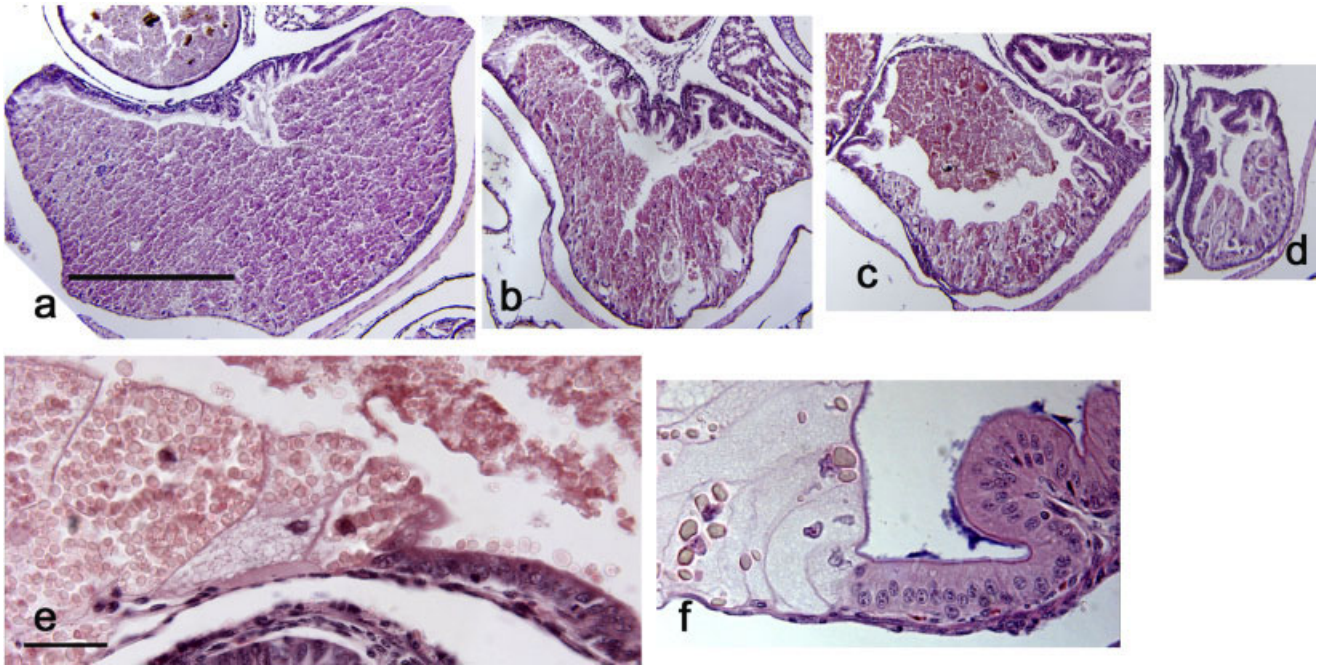

Fig. 4.

Fig. 4. Loss of yolky endoderm. a–d: Cross-sections through the small intestine at different stages of yolk resorption. This series is from *Eleutherodactylus planirostris*, and similar observations for *E. coqui* indicate this pattern of yolk resorption may be general for the entire genus. **a:** After hatching, much of the peritoneal cavity is still filled with yolk, and the dorsal margin of the entire small intestine is soon replaced with epithelium. **b:** As the epithelium replaces the yolky endoderm in a dorsal to ventral direction around the tube, the thickness of the yolky endoderm decreases as well as the intestine diameter. Note that the epithelial layer is multiply folded as it progresses ventrally. **c:** As the multiply folded epithelium continues to expand, most yolk platelets have been resorbed, but the depleted yolky endoderm cells are still present. **d:** Near the end of resorption, only a few remaining endoderm cells have yolk, whereas the majority of the surface is now intestinal epithelium. Figures e,f, from *E. coqui*, show that the boundary between intestinal epithelium and yolky endoderm cells is sharp. Note that these two cell types have different cell staining characteristics and nuclear morphology. **e:** At TS 14, the yolky endodermal cells have many yolk platelets. **f:** The boundary remains distinct even with near complete yolk resorption. Scale bar = 0.5 mm in a–d; 10 μm in e,f.

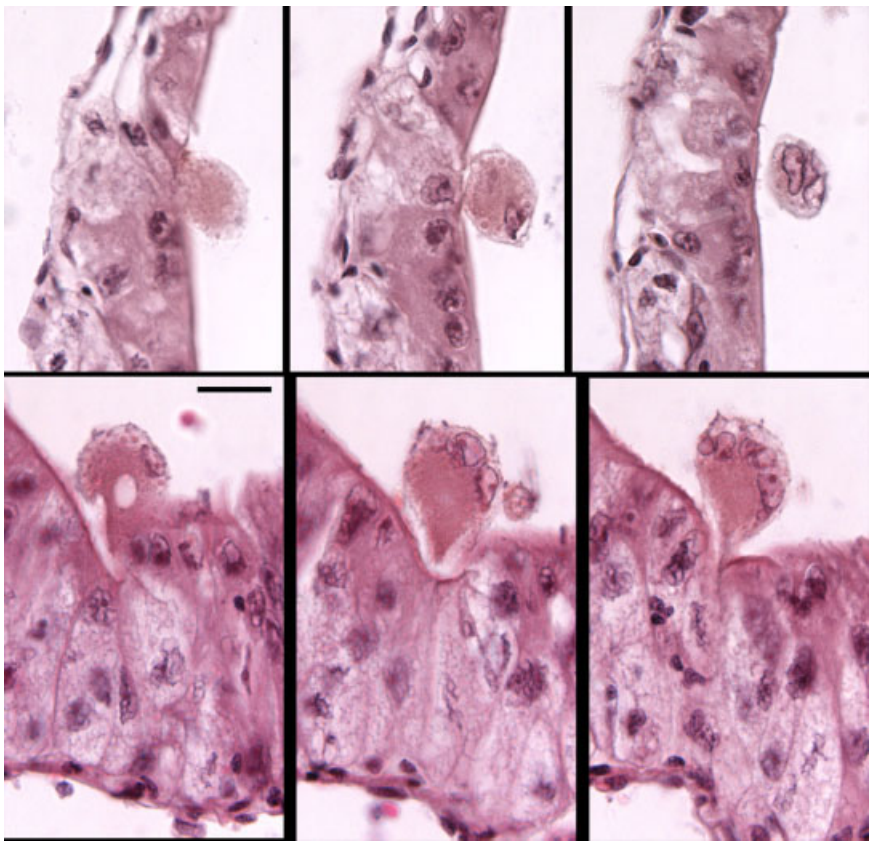

Fig. 5. Sloughing of depleted yolky endoderm cells. The top three panels show serial sections of a large yolky endoderm cell appearing to come out of the cell layer and into the lumen. The bottom three panels are another example. Multiple profiles of nuclei indicate that the sloughed cells may be multinucleated. Scale bar = 10 μm in all panels.

COLOR

the oldest at 27 days posthatch, and will be described later. The labeled yolky endoderm was sharply delineated from the more dorsal endodermal tissue, which was unlabeled (Fig. 7a). As the amount of yolk decreased, the region of labeling decreased, with-

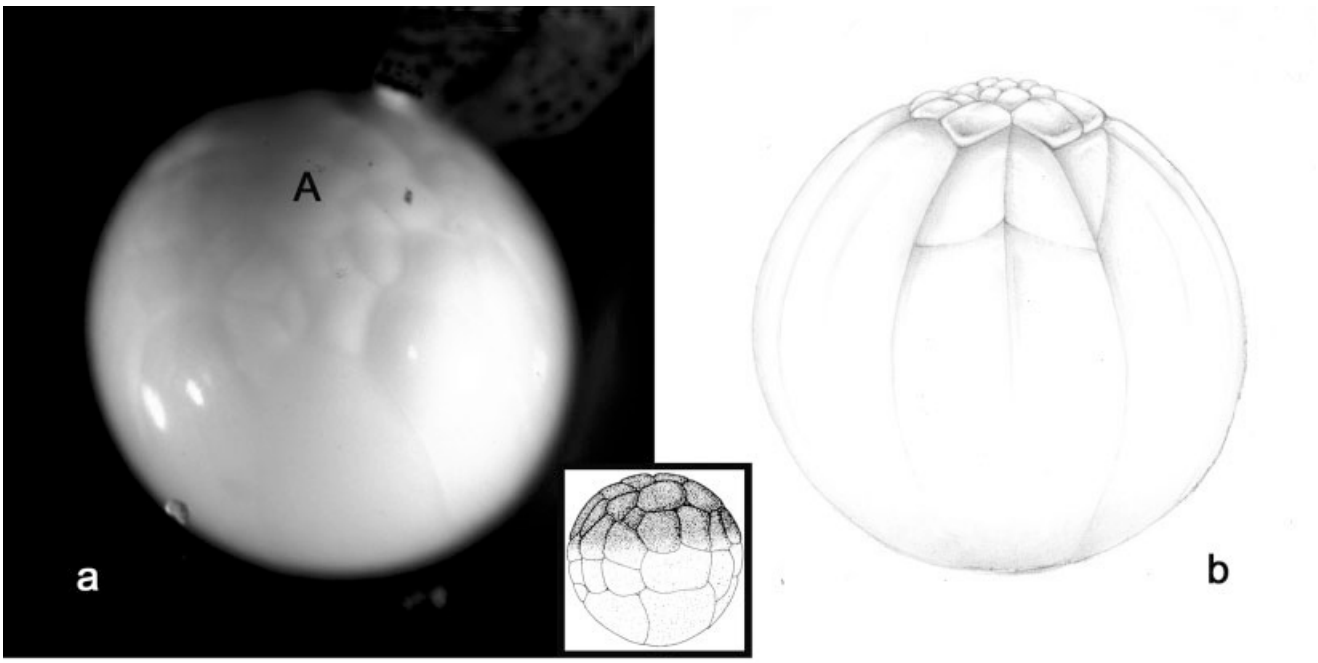

Fig. 6. *Eleutherodactylus coqui* morula. **a:** The *E. coqui* morula has a cap of small cells at the animal pole (A) and very large vegetal cells. There is a distinct boundary between the small animal cells and the larger vegetal ones. The animal pole is tilted forward in this photograph, so the full extent of the vegetal cells cannot be appreciated. **b:** This drawing of an ~40-cell morula shows the relationship between the animal cap of small cells and the very large vegetal cells. A few intermediate sized cells are forming at the boundary. The vegetal furrows are indistinct but extend to the vegetal pole. The inset shows a ~48 cell *X. laevis* morula, at the same scale as the *E. coqui* morula in (a) and (b). The size disparity between animal and vegetal cells is clearly less than in *E. coqui*. Reproduced with permission from Nieuwkoop and Faber (1956).

out label appearing in the more differentiated intestinal tissue (Fig. 7b). In the third week posthatching, the last of the label was found in the intestine (Fig. 7c), and a few froglets near the end of the third week had only a few fluorescent specks remaining. At this time, label was also found in the cloaca (Fig. 7c) and in the mesonephros (Fig. 7d). The label in the cloaca was dull and diffuse and associated with the wastes accumulated there (Fig. 7c). The only froglet that survived longer (27 days) had no yolky cells left and no label in any part of the gut, but its mesonephros was labeled.

At the 40- to 60-cell stage, there is a cap of smaller animal cells as well as a few intermediate-sized cells at the boundary between the small animal cells and the huge vegetal ones (Fig. 6). To ensure that descendants of cells labeled at the 40- to 60-cell stage retained label, FDA was injected into animal and intermediate cells. When the embryos were raised to froglets and dissected, label was found in many different tissues including spinal cord, vertebrae, and intestine (Fig. 7e–h). These results show that the label persisted for at least 2 weeks posthatching. Although we have not completely fate mapped the embryo, the presence of label in differentiated intestinal tissue shows that these tissues arise from more animal positions.

Labeling in Pronephros and Mesonephros

Apart from yolky endoderm, the only organs labeled in the entire body of the froglets, injected with FDA into the large vegetal cells, were the pronephros or mesonephros. Over half of the embryos at TS 9 to TS 15 showed distinct labeling in pronephros (7 of 13). Frogs after TS 15 showed no pronephric labeling, corresponding to the eventual disappearance of this structure. Disappearance of dye in pronephros was coupled with the gradual appearance of label in mesonephros. There was no mesonephric labeling in the TS 9 (n = 2) and TS 11 (n = 2) embryos, but label started appearing weakly as early as TS 13 (n = 4). At TS 15, two of five embryos had weak labeling in mesonephros, but labeling was strong in froglets up to 3 weeks posthatching (36 of 37), corresponding to the period when most of the yolky endoderm disappears (Fig. 7d). This finding includes the oldest froglet at 27 days that did not have label in its gut. These results suggest that the FDA was accumulating, due to clearance from the blood after the utilization of the labeled yolky endoderm.

Expression of *EcSox17*

In an attempt to follow the molecular development of the endoderm in *E. coqui*, we chose the transcription factor *Sox17*. Based on expression pattern, overexpression, and deficiency phenotypes, *Sox17* is a key regulator of endoderm development in *X. laevis*, mouse, and zebrafish (Hudson et al., 1997; Stainier, 2002; Shivdasani, 2002; Lewis and Tam, 2006; Dickinson et al., 2006). *Sox17* in *X. laevis* is a member of a proposed core autoregulatory network required for endoderm (Sinner at al., 2006).

Our *EcSox17* cDNA (accession no. EF397004) consists of a 36-nucleotide (nt) 5′-untranslated region (UTR), 1,143-nt open reading frame (ORF),

and 363-nt 3′-UTR, ending in a polyA tail. Comparing to *Sox 17*'s in *X. laevis*, the nucleotide sequence of the ORF is 68% identical to *XSox17α1*, 53% identical to *XSox17α2*, and 48% identical to *XSox17β*, and the amino acid sequence identities are 69%, 66%, and 45%, respectively. The HMG Box, nucleotides 211–417, is 82% identical to the *XSox17α1* HMG Box domain. The EcSox17 HMG domain is virtually identical at the amino acid level to other vertebrate Sox17 HMG domains, e.g., 89% with zebrafish, 95% with human, and 97% with *XSox17α1*.

In situs of *EcSox17* RNA in gastrulae showed nice staining vegetal to the blastoporal lip, but not in the rest of the vegetal region, as expected (Fig. 8a). When gastrulae were cut sagittally, staining was found on the involuted cells, which will line the archenteron (Fig. 8c). The large yolky cells, now directly exposed to the probe, still did not stain.

Although these patterns suggested that *EcSox17* is expressed only at the surface of the embryo near the blastoporal lip, in situs of *Sox17* in yolk-rich regions of *X. laevis* can give false-negative reactions (D'Souza et al., 2003). To test whether *EcSox17* RNA is present in the yolk-rich region, *E. coqui* gastrulae, equivalent to Nieuwkoop and Faber stage 10, were dissected into dorsal and ventral marginal zones and the yolky core (Fig. 9a,b). RNA was isolated from pooled pieces, and examined for the presence of *EcSox17* and *EcBra* RNA by reverse transcriptase-polymerase chain reaction (RT-PCR). *EcBra* is expressed in the prospective mesoderm as in other vertebrate embryos (Ninomiya et al., 2001), and *EcBra* expression in the marginal zone was confirmed (Fig. 9). Expression was absent in the vegetal core in two cases and present at a low level in one case, similar to our previous report (Ninomiya et al., 2001). In contrast, *EcSox17* RNA was found in both the marginal zones and in the vegetal core (Fig. 9). Neither *EcSox17* nor *EcBra* RNA was detected in samples without reverse transcription. Detection of *EcSox17* RNA by RT-PCR suggests that *EcSox17* RNA cannot be used to distinguish the endoderm forming near the blastoporal lip from that forming from the yolk-rich vegetal core.

The *EcSox17* RNA, detected in the vegetal core, is likely in part maternal in origin. *EcSox17* RNA was found in RNA from early cleaving embryos and from ovarian oocytes by RT-PCR (data not shown). Also, in our re-cloning of *EcSox17* cDNA from Hawaiian *E. coqui*, ovarian RNA was used as mentioned in the Experimental Procedures section.

Effect of Vegetal Cleavage Inhibition

The yolky endoderm cells appear to be playing mainly a nutritional role. This finding raises the question whether cleavage of these cells is necessary for development to proceed. To answer this question, we used the cell cycle regulator *c-mos*, which can arrest blastomeres in *X. laevis* embryos at metaphase (Sagata et al., 1989; Yew et al., 1991; Masui, 2000). Accordingly, one or more blastomeres of *E. coqui* cleaving embryos were injected with *c-mos* RNA. Although the mitotic stage was not checked, large areas of vegetal surface remained uncleaved 1 day later, when embryos were blastulae. When cleavage of a large vegetal blastomere at the 60- to 100-cell stage was inhibited, the embryo succeeded in gastrulation. The blastopore closed, excluding a large amount of yolk (Fig. 10a,b). Despite this loss, patterning of the embryo's body was normal as indicated by a head with eyes and the fore- and hindlimb buds (Fig. 10b,c). Embryos with reduced yolk could develop normally to become smaller than normal prefeeding frogs (Fig. 10d).

When vegetal cells of embryos a few divisions later were injected with *c-mos* RNA, the embryos internalized all of the yolky cells at gastrulation and continued development. Large uncleaved blastomeres were present among the cells of the gut (compare Fig. 11a vs. 11b). These included cases where the uncleaved blastomere extended ventrally from the floor of the archenteron (Fig. 11c). This position is expected from fate mapping, because the vegetal surface of the cleaving embryo ends up as the archenteric floor.

We succeeded in raising a few *mos*-injected embryos to a time when the control froglets had used up most of their yolk. Five of six had a large amount of amorphous debris in their gut lumen (Fig. 11d), with debris pushed into the stomach and the hindgut. This appearance indicates poor utilization of the yolk.

DISCUSSION

The treatment of yolk is fundamentally different between the amphibians and the amniotes, such as reptiles and birds. In amphibians, yolk in the form of yolk platelets is incorporated into cells. These cells later become tissues of the embryo. In amniotes, the large mass of yolk is not incorporated into cells. The yolk is broken down and moved into the developing embryo by means of the blood vessels of the yolk sac, which surrounds the uncleaved yolk. The evidence that we present here suggests that an intermediate state is present in the direct developing frog *E. coqui*. The yolk is compartmentalized into cells, but those cells do not contribute to the tissues of the froglet.

Evidence for Nutritional Endoderm in *E. coqui*

Several lines of evidence suggest that the yolky endoderm cells serve only a nutritional role. The gut of the hatched froglet consists of two grossly different tissues. These are the translucent tissues, forming the differentiating stomach and hindgut, and the yolky endoderm. The junction between these two tissues, especially along the dorsal side, is distinct, and this sharp distinction is emphasized by histological examination. One possibility is that the junction is where yolky endoderm cells differentiate into functional intestinal cells, but histology suggests otherwise. Even when depleted of yolk, the formerly yolky cells at the junction remain large and undifferentiated. Sloughing of these cells into the lumen is often detected.

Fate mapping provides further evidence for loss of the yolky cells, rather than differentiation. The yolky cells were strongly labeled by injection of FDA into large vegetal cells. If the yolky cells later differentiate, label should be found in the differentiated gut tissues, as the mass of yolky cells decreased. This transition did not occur. Rather, with the disappearance of

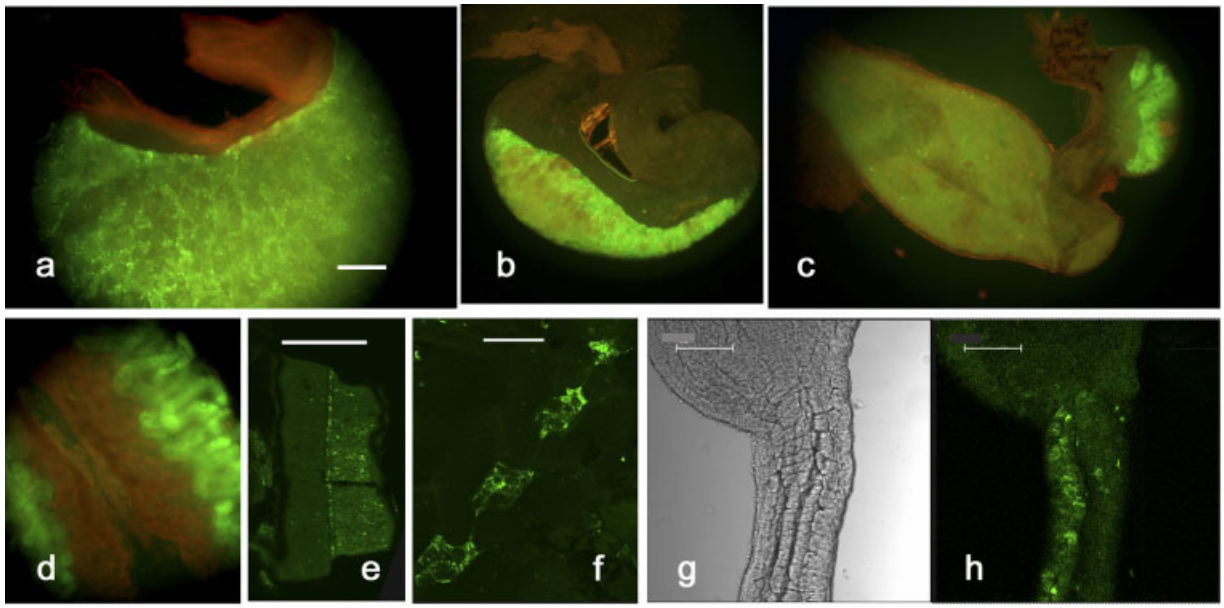

Fig. 7.

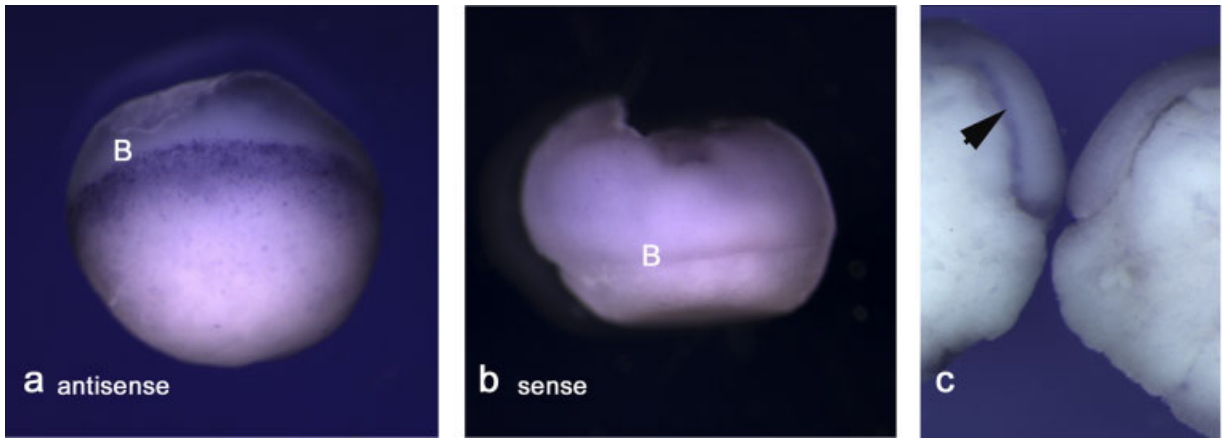

Fig. 8.

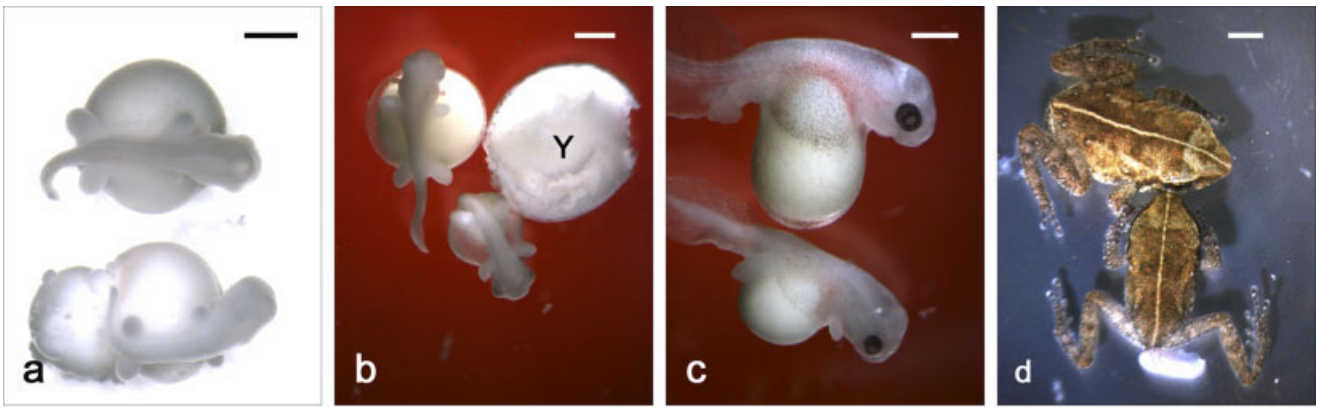

Fig. 10.

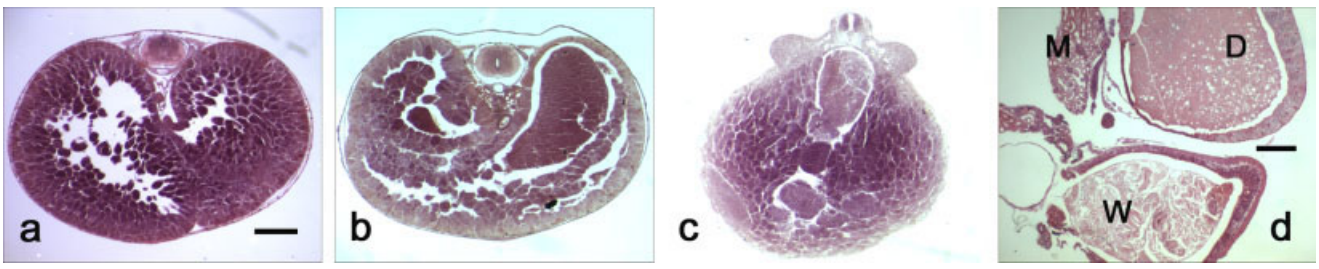

Fig. 11.

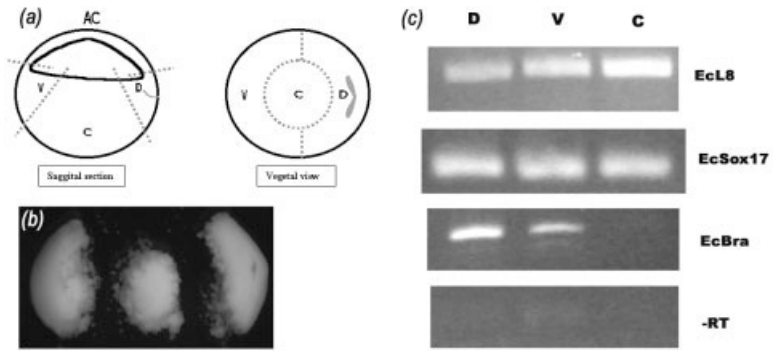

Fig. 9. *EcSox17* reverse transcriptase-polymerase chain reaction (RT-PCR) of gastrula. **a:** Early gastrula embryos were dissected into three pieces: dorsal marginal zone (D), ventral marginal zone (V), and vegetal core (C) as indicated in the diagrams of a sagittal section and a ventral view. **b:** This photograph of a dissected embryo shows three pieces, corresponding to the diagram of the vegetal view. Note the dorsal lip of the blastopore on the piece of dorsal marginal zone. **c:** RT-PCR was carried out on RNA isolated from pooled samples of the three pieces: dorsal, ventral, and core. *EcSox17* RNA was detected in all pieces. *EcBra* RNA, a mesodermal marker, was detected in the dorsal and ventral pieces, but not in the core. *EcL8* RNA, which codes for a ribosomal protein was used as a loading control. No amplification occurred in the absence of reverse transcription (−RT).

the yolky cells, label was detected in mesonephros and cloaca. Mesonephric labeling indicates that FDA was being cleared from blood. This finding may reflect uptake of FDA into circulation upon death of the labeled cell. Alternatively, the FDA may be taken into circulation along with yolk-derived metabolites, and then filtered out in the mesonephros. The strong labeling of the mesonephros indicates that the FDA is trapped there.

There are alternative explanations for the cloacal labeling as well. Hatched froglets use yolk for 1–2 weeks before they start eating. During this time, the cloaca is often swollen with waste. One possibility for the presence of FDA in the wastes is that a small amount of FDA is moved from the mesonephros through the mesonephric duct to the cloaca. A second possibility is that FDA is included in the wastes as the labeled yolky cells break down. A resolution between these alternatives may come by observing the path of FDA, injected directly into blood. The histological images of cells, apparently entering the lumen of the gut, along with detection of FDA in the cloacal wastes strongly suggests that the fate of the large yolky cells is death.

We attempted to show death directly by TUNEL labeling, but no labeled cell nuclei were observed. Apoptotic epithelial cell death in the remodeling intestine of *X. laevis* is associated with an increase in thyroid hormone, either added to the rearing water or endogenous thyroid hormone during natural metamorphosis and is detectable above background levels for only 2–3 days (Ishizuya-Oka, 1996). In the case *E. coqui*, loss of yolky endoderm cells begins after the thyroid hormone peak (see below) and occurs gradually over a period of 2–3 weeks, where there may not be a burst of cell death that is detectable above the background levels. Also, changes in nuclear histology associated with

Fig. 7. Fate mapping. **a:** This gut, isolated from a froglet injected with fluorescein dextran amine (FDA) into a vegetal cell, still has a lot of yolk. The large yolky cells fluoresce green while the more differentiated gut tissues lack fluorescence and appear orange. **b:** There is less yolk in this gut. Again the large yolky cells fluoresce green and the rest of the tissues show little fluorescence. The lack of fluorescence in the differentiated tissues indicates that green yolky cells do not subsequently become intestinal tissues. **c:** This gut has very little yolk left, visible as the intense green stain on the right side. The more diffuse green stain on the left is material within the cloaca, which will be defecated. **d:** This mesonephros is from the same froglet as Figure 7c. There is a lot of FDA present, which is likely due to the attempt of the froglet to excrete the dye, which was filtered from the blood. This mesonephric staining was generally not found in embryos, sacrificed with more yolk present. **e:** This spinal cord was isolated from a froglet that was injected with FDA into a cell near the animal pole. Label is present on one side only. **f:** This froglet was also injected with FDA into an animal cell, and label is present in vertebrae. **g,h:** Phase (g) and fluorescent confocal (h) views of the junction between the stomach and the intestine in a froglet that was injected with FDA into an intermediate sized cell. Labeled cells are present in the intestine but not the stomach. Scale bar = 0.5 mm in a–c, 300 μm in e, 150 μm in f,g,h.

Fig. 8. *EcSox17* in situ hybridization of gastrula. **a:** Cells vegetal to the blastoporal lip (B) express *EcSox17*. **b:** No signal is present with a sense probe. **c:** To reveal internal expression, gastrulae were bisected, before in situ hybridization. With an antisense probe (left), the large mass of yolky cells is unstained, and staining is present along the involuted cells (arrowhead) that will line the archenteron. There is no staining of these cells with the sense probe (right).

Fig. 10. Vegetal cleavage inhibition at 60- to 100-cell stage. *Mos* RNA was injected into a large vegetal blastomere at the 60- to 100-cell stage, and the embryos were raised. **a:** A *mos*-injected embryo (bottom) is compared with a normal TS5 embryo (top). The *mos*-injected embryo failed to incorporate all of the yolk. Nonetheless, the embryo has a normal anterior–posterior axis as indicated by the presence of all forelimbs and hindlimbs. **b:** A normal TS 6 embryo (left) is shown next to a *mos*-injected embryo (bottom). The injected embryo has a normal head and limbs, but lacks most of its yolk (Y). **c:** A normal TS 9 embryo (top) is compared with a *mos*-injected embryo (bottom), which has a small supply of yolk. **d:** A froglet (bottom), derived from a *mos*-injected embryo that had lost a lot of yolk, is much smaller than its normal sibling. The *mos*-injected embryo has not finished absorbing its tail. Scale bars = 1 mm.

Fig. 11. Vegetal cleavage inhibition at the ~200-cell stage. *Mos* RNA was injected into a large vegetal blastomere a few divisions later than in Figure 10. **a:** A section through a control TS 12 embryo shows many large endodermal cells. The spaces are artifacts. **b:** A section through a *mos*-injected embryo shows the presence of several huge, uncleaved vegetal cells in the endoderm. **c:** Another example of a *mos*-injected embryo shows several huge, uncleaved cells, including one that extends to the floor of the archenteron. Note the limb buds. **d:** This section shows the gut of a *mos*-injected embryo that developed to a froglet. There is a large mass of debris (D) in the intestinal lumen, as well as wastes (W) in the cloaca. Mesonephros (M). Scale bar = 0.5 mm in a–c, 0.25 mm in d.

apoptosis in *X. laevis*, including chromatin condensation and nuclear break up (Ishizuya-Oka and Ueda, 1996), are not observed in *E. coqui*. Even when the yolky endoderm cells are being extruded into the lumen, the nuclear structure is intact, lacking any histological indications of apoptosis. Therefore, death of the yolky endoderm cells appears not to be by apoptosis and occurs after extrusion into the lumen.

Comparison Between *E. coqui* and *X. laevis*

Yolk platelets are present throughout the cytoplasm of the fertilized *X. laevis* egg (Danilchik and Gerhart, 1987; Danilchik and Denegre, 1991). All cells inherit yolk, which is metabolized within the embryonic cells. In birds, this metabolism within cells occurs, but in addition, the uncleaved yolk is broken down, moved into the yolk sac endoderm, and distributed by means of the blood to the growing embryo (Bellairs, 1964; Yoshizaki et al., 2004). This second utilization of yolk likely occurs in *X. laevis*, although this use does not appear to be documented. The *X. laevis* endodermal cells are yolk-rich, and this yolk is consumed before initiation of feeding by the tadpole. Some of the metabolites from these endodermal yolky cells likely enter circulation to supply nutrition to the rest of the embryo. A simple test of this possibility is to see whether the dry mass of the embryo, minus the gut, increases as the yolk is used between stages NF 41 and 46.

When fate mapping is done, all regions of the endoderm in a *X. laevis* neurula contribute cells to the differentiated tadpole intestine (Chalmers and Slack, 2000). This result suggests that a nutritional endoderm, as we have documented for *E. coqui*, does not exist in *X. laevis*. The fate mapping, however, is not sufficiently detailed to determine the fate of each individual cell. It is possible that a fraction of the *X. laevis* endodermal cells die after depletion of their yolk, and these cells would be equivalent to the nutritional endoderm in *E. coqui*. Alternatively, the *X. laevis* embryo must generate a very long coiled gut in a short amount of time (Chalmers and Slack, 1998), so all of the endodermal cells may use their yolk supply for rapid division and differentiation.

Expression of *EcSox17*

Zygotic expression of *X. laevis Sox17* depends on the maternally expressed transcription factor *VegT* and Nodal ligands, activated by VegT (Yasuo and Lemaire, 1999; Xanthos et al., 2001). RNA for *EcVegT*, the *E. coqui* orthologue, is greatly enriched near the animal pole of the *E. coqui* oocyte and cleaving embryo, unlike the localization of *VegT* RNA to the vegetal cortex of the *X. laevis* oocyte (Beckham et al., 2003). Nodal signaling in the *E. coqui* embryo, as assayed by mesoderm inducing activity, is restricted to the surface cells of the early gastrula (Ninomiya et al., 2001). It is not present at the vegetal pole or in the deep cells extending from the vegetal pole to the blastocoele floor.

We, therefore, expected *EcSox17* expression to be limited to the equatorial surface and to be absent from the vegetal pole and the vegetal core. This expected absence of *EcVegT* expression would correspond to the nutritional endoderm, whose fate is to degenerate rather than to differentiate as intestinal tissues. Although in situ patterns of *EcSox17* RNA fit these expectations, RT-PCR of isolated vegetal cores demonstrated the presence of *EcSox17* RNA there. This result raises questions of the origin and function of *EcSox17* RNA in the vegetal core. With respect to origin, some of the *EcSox17* RNA is maternal, an expression not present in *X. laevis* (Hudson et al., 1997). One possibility is that zygotic signaling is very inefficient when cells are so big and yolky, so the large vegetal cells in *E. coqui* may not be able to rely on a zygotic source of any necessary RNAs. This speculation then begs the question as to why any RNA is necessary for cells, which serve only a nutritional function and are scheduled to die. Nonetheless, these cells survive for more than a month, and they must deliver metabolites of yolk to the embryo. Further analysis of gene expression of the nutritional endoderm would help in a further understanding of the nature of these cells.

Relationship Between Thyroid Hormone and Intestinal Development

In all frogs studied to date, thyroid hormone (TH) is required for intestine remodeling from the larval form to the adult version (Shi, 2000). Our analysis of gut development in *E. coqui* suggests biphasic intestinal development with respect to TH. In *X. laevis*, intestinal remodeling occurs in a sequence of events preceded by limb outgrowth and followed by tail resorption. All of these events, as well as other organ transformations, require TH, which reaches a peak in blood concentration when the tail begins resorbing. In *E. coqui*, intestinal remodeling of the anterior part from a simple tube to the multiply folded adult form is complete by TS 15 before hatching. This remodeling occurs in the same sequence as in *Xenopus*, that is, limbs, intestine, and then tail. At this point, most of the yolky endoderm is still present, and then over the next 6–8 days after hatching and tail resorption, the yolky endoderm is replaced by an epithelium in what can be considered a second phase of postembryonic intestinal development.

Unlike in *X. laevis* and other frogs, the role played by TH in intestinal development in *E. coqui* is unclear. Direct measurements of TH across development have not been carried out, but the beginning of endogenous TH production is predicted to be around TS 11, just after the thyroid gland forms (Jennings and Hanken, 1998) and when TH-dependency begins (Callery and Elinson, 2000; Callery et al., 2001). The peak histological activity of the thyroid gland and beginning of tail resorption occurs at TS 13 (Jennings and Hanken, 1998, Townsend and Stewart, 1985), suggesting the peak of endogenous TH titer at this stage. However, peak TH levels may occur after hatching because TH receptor beta (TRβ) expression, which is presumably correlated with TH titers as in *X. laevis* (Shi and Brown, 1993; Shi, 1994), continues to increase after hatching (Callery and Elinson, 2000). Thus, TH is likely present during prehatching and potentially involved in intestinal remodeling of the anterior tube, and the high TRβ expression posthatching suggests high TH levels

even after hatching during yolky endoderm replacement. Future hormone measurements and endocrine experiments are required to determine the role of TH in *E. coqui* intestinal development.

Why Is Holoblastic Cleavage Conserved in Amphibians?

The amniote egg was a key innovation in the evolution of terrestrial vertebrates, the tetrapods. Eggs of extant amphibians and amniotes differ in three main ways. First, the amniote egg generates a set of extraembryonic membranes, the amnion, chorion, allantois, and yolk sac, which the amphibian egg does not. Second, the maximum size of an amphibian egg is approximately 1 cm in diameter, while eggs of turtles, lizards, snakes, and birds, are generally much larger. Third, amphibian eggs divide holoblastically, while amniote eggs, except for the small eggs of marsupial and placental mammals, divide meroblastically.

Many hypotheses have been proposed for the origin of the extraembryonic membranes. The two hypotheses under most active current consideration are that the membranes were originally used to permit terrestrial development and that the membranes were originally used to mediate maternal exchange for an embryo developing within the mother's body. Vigorous attempts have been made to use phylogenetic methods to decide between these hypotheses, but these attempts have not produced a resolution (Laurin and Reisz, 1997; Wilkinson et al., 2002; Laurin, 2005). On the other hand, there is general consensus on biological and phylogenetic grounds that the eggs of the original tetrapods were much like those of extant amphibians and cleaved holoblastically (Romer, 1957; Goin and Goin, 1962; Carroll, 1969, 1970; Elinson, 1987, 1989; Collazo et al., 1994; Packard and Seymour, 1997; Arendt and Nübler-Jung, 1999; Elinson and Beckham, 2002; Chea et al., 2005). A transition to meroblastic cleavage would be one of the conditions, along with provision for gas exchange, which permitted the great increase in yolk content and egg size, found in the amniotes.

Based on phylogenetic analysis, Collazo et al. (1994) proposed that a transition from holoblastic to meroblastic cleavage occurred five times in the chordates. The only instance of a meroblastic to holoblastic transition is within mammals. All amphibians have holoblastic cleavage (Elinson, 1987). Chipman et al. (1999) called cleavage in *Hyperolius puncticulatus* "pseudo-meroblastic," because the yolk-rich vegetal cells appeared to be so large. Their observations were based on fixed embryos, however, in which cell boundaries among yolk-rich cells may be obscured. It would be worth examining living embryos of *H. puncticulatus* and related Hyperolidae with larger eggs to see if there are any exceptions to the holoblastic rule. The conservation of amphibian holoblastic cleavage raises the question as to why there has been no second viable origin of meroblastic cleavage among tetrapods in the past 360 million years.

Given the presence of nutritional endoderm in *E. coqui*, we asked whether cleavage of the yolky vegetal region of the egg is necessary. Inhibition of early vegetal cleavage led to a failure to incorporate all of the yolk at gastrulation. Nonetheless, the embryos closed the blastopore and had normal patterning of the anterior–posterior axis. When vegetal cleavage was inhibited a few divisions later, all of the yolky cells, including large uncleaved ones, were internalized during gastrulation. In *X. laevis*, yolky vegetal cells actively participate in the rearrangements during gastrulation in a movement called vegetal rotation (Winklbauer and Schurfield, 1999; Ibrahim and Winklbauer, 2001). It is not known whether vegetal rotation occurs in *E. coqui*, but it is unlikely to be required, given the closure of the blastopore in *E. coqui* embryos with huge cleavage-inhibited cells. The morphology of gastrulation is different between amphibians and amniotes, and Arendt and Nübler-Jung (1999) hypothesized that differences in gastrulation movements evolved in conjunction with the presence of an uncleaved yolk mass. Nonetheless, our results indicate that the amphibian pattern of gastrulation movements does not require complete cleavage of the vegetal region into small cells.

In amniotes, the yolk is enveloped by the yolk sac after gastrulation. In *E. coqui*, the yolky cells are secondarily enveloped by the body wall, which brings musculature from the somites to the ventral midline (Elinson and Fang, 1998). Although the movement of the body wall in *E. coqui* is superficially similar to that of the yolk sac, it is not homologous. The body wall includes somitic mesoderm rather than the splanchnic mesoderm of the lateral plate, and it does not include the endoderm. Nonetheless, the similarity suggests that the independent evolution of an enveloping layer can occur, and it could be used to surround an uncleaved yolk mass. Neither the amphibian gastrulation pattern nor the lack of a yolk enveloping layer appears to preclude a transition to meroblastic cleavage.

We managed to raise a few embryos with internalized large yolk cells to froglets, and these animals had a large amount of debris in the lumen of the gut. The debris spread from the intestine into the stomach. These difficulties in using the yolk from the large uncleaved cells suggest that the membranes of the yolky endoderm cells in amphibians may function in yolk metabolism, either its breakdown or its transport. Perhaps this function would have to be acquired by another tissue, such as the amniote's yolk sac, before cleavage of the yolky region could be abandoned.

EXPERIMENTAL PROCEDURES

Animals and Embryos

Adult *E. coqui* were collected in Puerto Rico under permits issued by the Departmento de Recursos Naturales y Ambientales and in Hawaii under Injurious Wildlife Export Permits issued by the Department of Land and Natural Resources. A reproductive colony was maintained at Duquesne University, and adults and embryos were treated according to protocols approved by the Institutional Animal Care and Use Committee.

All embryos were obtained from natural matings within our laboratory colony (Elinson et al., 1990). After the

fertilized eggs were laid, they were removed from the guarding male and kept in a moist chamber. When embryos reached a desired stage, they were submerged in 20% Steinberg's solution (12 mM NaCl, 0.134 mM KCl, 0.068 mM $Ca(NO_3)_2$, 0.166 mM $MgSO_4$, 1 mM Tris HCl, pH ~6.5) to allow the jelly capsule to swell. The jelly capsule, consisting of three jelly layers, and the fertilization envelope were removed using watchmaker's forceps, depending on the use of the embryos. While it is relatively easy to do this on embryos that have completed neurulation, other treatments were used for earlier embryos with tighter fertilization envelopes. After removing the outer and middle jelly layers of the earlier embryos with forceps, the inner jelly layer was dissolved with 2.5% cysteine, pH 8.0, by gently swirling for 5–8 min. Embryos were thoroughly rinsed and then raised in 20% Steinberg's solution. To weaken the fertilization envelope, dejellied embryos were further treated with 2.5% cysteine, 2% papain, and 2% α-chymotrypsin, pH 8.0, for 10–20 sec (Hennen, 1973). The embryos were washed with 20% Steinberg's solution and transferred to 1% bovine serum albumen in 100% Steinberg's solution. The fertilization envelope was removed carefully with forceps.

The stage of development was determined according to the table by Townsend and Stewart (1985). Each stage is denoted "TS number," ranging from TS 1, the cleaving embryo, to TS 15, the hatched froglet. The hatched froglet has a large mass of yolky cells, and the yolk is used over the next 1–2 weeks. Developing guts after hatching were compared based on the amount of yolk remaining.

In addition to *E. coqui* embryos, a few embryos of *Eleutherodactylus planirostris*, collected in Tallahassee, Florida, were examined. This species is closely related to *E. coqui*. They have the same nesting ecology and progress through the same developmental stages.

Histology

Embryos or isolated guts were fixed in Smith's fixative (Rugh, 1962) or 4% paraformaldehyde in phosphate buffered saline, pH 7.4 (PFA). The former was generally used for younger embryos with a lot of yolk, whereas the latter was used for isolated later guts with reduced yolk. Embryos were anesthetized in 0.05% Tricaine methanesulfonate (MS222), buffered to pH 7.3 by the addition of solid Na_2PO_4, and guts were dissected in 200% Steinberg's solution. For fixation using Smith's fixative, equal parts of two stock solutions were mixed fresh for use, and embryos were fixed in the dark. Smith's Stock A is 1% potassium dichromate ($K_2Cr_2O_7$), and Smith's Stock B is a 5% acetic acid, 7.4% formaldehyde. After fixation, the embryos were rinsed with water and stored in buffered 3.7% formaldehyde at room temperature. For fixation using PFA, guts were fixed for 2 hr and then stored in 70% ethanol at room temperature or 100% ethanol at −20°C. Fixed guts were then dehydrated and infiltrated with paraffin in an Excelsior ES tissue processor (Thermo Electron Corp.) before embedding in paraffin blocks. They were sectioned at 8 μm and dried onto Probe-On Plus microscope slides (Fisher). For histological staining, sections on slides were rehydrated, stained with hematoxylin and eosin, dehydrated, and then mounted with Permount (Fisher). Digital pictures were taken using a Microprocessor digital camera (Q-Imaging) on an Olympus compound microscope.

Lineage Tracing

After removal of their outer and middle jelly layers, embryos with 40–60 cells were partially submerged in 5% Ficoll prepared in 100% Steinberg's solution. One large vegetal blastomere was injected with 9.2 nl of 50 mg/ml FDA (10,000 molecular weight, anionic, lysine fixable, Molecular Probes), using a Drummond Nanoject Variable Automatic Injector. Injected embryos were cultured individually in 5% Ficoll in 100% Steinberg's solution with 50 μg/ml gentamicin overnight and then placed in 20% Steinberg's solution, which was changed regularly.

When the embryos or froglets reached the desired stage, they were anesthetized in 1% MS 222 in 100% Steinberg's solution for 4–5 sec and dissected in 200% Steinberg's solution. They were fixed in MEMFA (100 mM MOPS, 2 mM EGTA, 1 mM $MgSO_4$, 3.7% formaldehyde, pH 7.4; Harland, 1991) and stored at 4°C. The fixed frogs were dissected further to separate different parts of the body, for example, foregut, hindgut, liver, mesonephros, heart, pronephros (if present), vertebrae, spinal cord, brain, eyes, forelimbs, and hindlimbs. Each separated part or organ of the frog body was mounted on a glass slide in a drop of anti-fade buffered glycerol (25 mg of n-propyl gallate, 5 ml of PBS, 5 ml of glycerol, pH 8.0–8.6). The mounted organs were covered with a cover glass, which was gently pressed down, and the slides were kept at 4°C. For controls, organs from uninjected froglets were processed in the same way.

The specimens were examined using a Nikon Microphot-SA microscope with fluorescence filters for fluorescein isothiocyanate (FITC). Confocal imaging was done using a Leica TCS SP2 Confocal Microscope. The wavelength was set at FITC WIDE and special FITC GREY, and the lasers were 488 Ar/ArKr set at minimum.

Cloning *EcSox17* cDNA

RNA was extracted from neurula and limb bud stages (TS 3–4) with Trizol (Invitrogen) and used to prepare cDNA. Degenerate primers, based on conserved *Sox17* sequences between *X. laevis*, zebrafish, mouse, and human, were used to amplify a 261-bp fragment by PCR. This fragment was cloned into a pGEM T-Easy vector. It had high sequence identity to *Sox17*'s in other species, so it was extended by 3′- and 5′-rapid amplification of cDNA ends to yield a consensus sequence of 1,565 nt, which contains the complete ORF for a 380 amino acid protein. Our *EcSox17* clones were derived from *E. coqui*, collected in Puerto Rico, but during the course of these experiments, our source of *E. coqui* changed from Puerto Rico to Hawaii. We recloned *EcSox17* from ovary of Hawaiian *E. coqui* by PCR, using exact primers, and sequencing confirmed that the two populations had the same *EcSox17*.

In Situ Hybridization

Dejellied embryos were fixed in MEMFA. After 3 hr, the fertilization

envelope was removed carefully with forceps. Bisection of embryos, if required, was done at this point with a razor blade. The embryos were fixed for a further 2 hr, washed twice in 100% ethanol, and stored at −20°C in 100% ethanol until further use.

EcSox17 cDNA was cloned into a pGEM-T EASY vector (Promega). The plasmid was cut with *Nco*I and transcribed with SP6 to produce the antisense probe, labeled with digoxigenin. The plasmid was cut with *Spe*I and transcribed with T7 to produce the sense probe. In situ hybridization was carried out with hydrolyzed probes according to standard procedures (Harland, 1991; Nath et al., 2005), which included a 20-min treatment of the fixed embryos with 10 μg/ml proteinase K. Hybridization was visualized by using BM Purple AP substrate (Roche) for alkaline phosphatase.

Dissection of Embryos and RT-PCR

Gastrulae were dissected into different pieces for RT-PCR. After removal of the jelly layers and fertilization envelope, the embryo flattened into the shape of a fat pancake. The embryo was positioned with a hair loop so that its vegetal half was up and the dorsal blastoporal lip was visible. Using fine tungsten needles, two incisions of equal length, extending toward the center of the embryo were made on opposite sides lateral to the dorsal lip (Fig. 9). The inner ends of the incisions were joined by cutting in a semicircular manner on either side of the central vegetal core. At the end of dissection, a semicircular dorsal piece with the dorsal lip, a semicircular ventral piece, and a central core of the early gastrula remained (Fig. 9). RNA was extracted from 8–10 dissected pieces or 4–5 whole embryos with Trizol.

cDNA for PCR was reverse transcribed from RNA using the M-MLV enzyme and oligo dT. Primers for *EcSox17* were as follows: Forward 5′-CTACAGCTTGCCTACACCTGA-3′ and Reverse 5′-CATCCCATCATACTCTGTGCA-3′. These primers amplify a 201-bp fragment. *EcL8*, a ribosomal protein gene that is expressed throughout development, was used a loading control. Primers for *EcL8* were published previously (Callery and Elinson, 2000), as were primers for the mesodermal marker *EcBra* (Ninomiya et al., 2001).

Cleavage Inhibition

The plasmid pX64, with the *X. laevis c-mos* coding region in pSP64 (Promega), was provided by Nick Duesbery, Van Andel Institute, Grand Rapids, MI. The pX64 plasmid was cut with *Bgl*I and transcribed with SP6, using the mMessage mMachine Kit (Ambion, Austin, TX). Cleaving *E. coqui* embryos were placed in 20% Steinberg's solution, and the outer jelly layers were removed with forceps. One or more blastomeres near the vegetal pole were injected with 9.2–36.8 nl of 200 ng/μl *c-mos* RNA using a Drummond Nanoject Injector, and the embryos were allowed to develop.

ACKNOWLEDGMENTS

We thank Kimberly Nath for technical assistance, Dr. Nick Duesbery (Van Andel Institute, Grand Rapids, MI) for the *c-mos* plasmid, Brian Storz for the gift of *E. planirostris*, and Robert Hogarth for the drawing of the *E. coqui* cleaving embryo.

REFERENCES

Arendt D, Nübler-Jung K. 1999. Rearranging gastrulation in the name of yolk: evolution of gastrulation in yolk-rich amniote eggs. Mech Dev 81:3–22.

Beckham YM, Nath K, Elinson RP. 2003. Localization of RNAs in oocytes of *Eleutherodactylus coqui*, a direct developing frog, differs from *Xenopus laevis*. Evol Dev 5:562–571.

Bellairs R. 1964. Biological aspects of the yolk of the hen's egg. Adv Morphog 4: 217–272.

Callery EM, Elinson RP. 2000. Thyroid hormone-dependent metamorphosis in a direct developing frog. Proc Natl Acad Sci U S A 97:2615–2620.

Callery EM, Fang H, Elinson RP. 2001. Frogs without polliwogs: evolution of anuran direct development. Bioessays 23: 233–241.

Carroll RL. 1969. Problems of the origin of reptiles. Biol Rev 44:393–432.

Carroll RL. 1970. Quantitative aspects of the amphibian-reptilian transition. Forma Functio 3:165–178.

Chalmers AD, Slack JMW. 1998. Development of the gut in *Xenopus laevis*. Dev Dyn 212:509–521.

Chalmers AD, Slack JMW. 2000. The *Xenopus* tadpole gut: fate maps and morphogenetic movements. Development 127:381–392.

Chea HK, Wright CV, Swalla BJ. 2005. Nodal signaling and the evolution of deuterostome gastrulation. Dev Dyn 234: 269–278.

Chipman AD, Haas A, Khaner O. 1999. Variations in anuran embryogenesis: yolk-rich embryos of *Hyperolius puncticulatus* (Hyperoliidae). Evol Dev 1:49–61.

Collazo A, Bolker JA, Keller R. 1994. A phylogenetic perspective on teleost gastrulation. Amer Nat 144:133–152.

Danilchik MV, Gerhart JC. 1987. Differentiation of the animal–vegetal axis in *Xenopus laevis* oocytes. I. Polarized intracellular translocation of platelets establishes the yolk gradient. Dev Biol 122:101–112.

Danilchik MV, Denegre JM. 1991. Deep cytoplasmic rearrangements during early development in *Xenopus laevis*. Development 111:845–856.

Dickinson K, Leonard J, Baker JC. 2006. Genomic profiling of Mixer and Sox17 β targets during *Xenopus* endoderm development. Dev Dyn 235:368–381.

D'Souza A, Lee M, Taverner N, Mason J, Carruthers S, Smith JC, Amaya E, Papalopulu N, Zorn AM. 2003. Molecular components of the endoderm specification pathway in *Xenopus tropicalis*. Dev Dyn 226:118–127.

Elinson RP. 1987. Change in developmental patterns: embryos of amphibians with large eggs. In: Raff RA, Raff EC, editors. Development as an evolutionary process. NY: Alan R. Liss, Inc. p 1–21.

Elinson RP. 1989. Egg evolution. In: Wake DB, Roth G, editors. Complex organismal functions: integration and evolution in vertebrates. Chichester, England: John Wiley & Sons. p 251–262.

Elinson RP, Beckham Y. 2002. Development in frogs with large eggs and the origin of amniotes. Zoology 105:105–117.

Elinson RP, Fang H. 1998. Secondary coverage of the yolk sac by the body wall in the direct developing frog, *Eleutherodactylus coqui*: an unusual process for amphibian embryos. Dev Genes Evol 208: 457–466.

Elinson RP, del Pino EM, Townsend DS, Cuesta FC, Eichhorn P. 1990. A practical guide to the developmental biology of terrestrial-breeding frogs. Biol Bull 179: 163–177.

Goin OB, Goin CJ. 1962. Amphibian eggs and the montane environment. Evolution 16:364–371.

Harland RM. 1991. In situ hybridization: an improved whole-mount method for *Xenopus* embryos. Methods Cell Biol 36: 685–695.

Hennen S. 1973. Competence tests of early amphibian gastrula tissue containing nuclei of one species (*Rana palustris*) and cytoplasm of another (*Rana pipiens*). J Embryol Exp Morphol 29:529–238.

Hudson C, Clements D, Friday RV, Stott D, Woodland HR. 1997. Xsox17α and -β mediate endoderm formation in *Xenopus*. Cell 91:397–405.

Ibrahim H, Winklbauer R. 2001. Mechanisms of mesendoderm internalization in the *Xenopus* gastrula: lessons from the ventral side. Dev Biol 240:108–122.

Ishizuya-Oka A. 1996. Apoptosis of larval cells during amphibian metamorphosis. Microsc Res Tech 34:228–235.

Ishizuya-Oka A, Ueda S. 1996. Apoptosis and cell proliferation in the *Xenopus* small intestine during metamorphosis. Cell Tissue Res 286:467–476.

Jennings DH, Hanken J. 1998. Mechanistic basis of life history evolution in anuran amphibians: thyroid gland development in the direct-developing frog, *Eleutherodactylus coqui*. Gen Comp Endocrinol 111:225–232.

Laurin M. 2005. Embryo retention, character optimization, and the origin of the extra-embryonic membranes of the amniotic egg. J Nat Hist 39:3151–3161.

Laurin M, Reisz RR. 1997. A new perspective on tetrapod phylogeny. In: Martin KLM, Sumida SS, editors. Amniote origins: completing the transition to land. San Diego: Academic Press. p 9–59.

Lewis SL, Tam PPL. 2006. Definitive endoderm of the mouse embryo: formation, cell fates, and morphogenetic function. Dev Dyn 235:2315–2329.

Masui Y. 2000. The elusive cytostatic factor in the animal egg. Nat Rev Mol Cell Biol 1:228–232.

Nath K, Boorech JL, Beckham YM, Burns MM, Elinson RP. 2005. Status of RNAs, localized in *Xenopus laevis* oocytes, in the frogs *Rana pipiens* and *Eleutherodactylus coqui*. J Exp Zool (Mol Dev Evol) 304B:28–39.

Nieuwkoop PD, Faber J. 1956. Normal table of *Xenopus laevis* (Daudin). Amsterdam: North-Holland Publishing Co. 243 p.

Ninomiya H, Zhang Q, Elinson RP. 2001. Mesoderm formation in *Eleutherodactylus coqui*: body patterning in a frog with a large egg. Dev Biol 236:109–123.

Packard MJ, Seymour RS. 1997. Evolution of the amniote egg. In: Martin KLM, Sumida SS, editors. Amniote origins: completing the transition to land. San Diego: Academic Press. p 265–290.

Romer AS. 1957. Origin of the amniote egg. Scientific Monthly 85:57–63.

Rugh R. 1962. Experimental embryology. 3rd ed. Minneapolis: Burgess Publishing Co. 501 p.

Sagata N, Watanabe N, Vande Woude GF, Ikawa Y. 1989. The c-mos proto-oncogene product is a cytostatic factor responsible for the meiotic arrest in vertebrate eggs. Nature 342:512–518.

Shi YB. 1994. Molecular biology of amphibian metamorphosis. Trends Endocrinol Metab 5:14–20.

Shi YB. 2000. Amphibian metamorphosis: from morphology to molecular biology. New York: Wiley-Liss. 288 p.

Shi YB, Brown DD. 1993. The earliest changes in gene expression in tadpole intestine induced by thyroid hormone. J Biol Chem. 268:20312–20317.

Shivdasani RA. 2002. Molecular regulation of vertebrate early endoderm development. Dev Biol 249:191–203.

Sinner D, Kirilenko P, Rankin S, Wei E, Howard L, Kofron M, Heasman J, Woodland HR, Zorn AM. 2006. Global analysis of the transcriptional network controlling Xenopus endoderm formation. Development 133:1955–1966.

Stainier DY. 2002. A glimpse into the molecular entrails of endoderm formation. Genes Dev 16:893–907.

Townsend DS, Stewart MM. 1985. Direct development in *Eleutherodactylus coqui* (Anura: Leptodactylidae); a staging table. Copeia 1985:423–436.

Wilkinson M, Richardson MK, Gower DJ, Oommen OV. 2002. Extended embryo retention, caecilian oviparity and amniote origins. J Nat Hist 36:2185–2198.

Winklbauer R, Schurfield M. 1999. Vegetal rotation, a new gastrulation movement involved in the internalization of the mesoderm and endoderm in *Xenopus*. Development 126:3703–3713.

Xanthos JB, Kofron M, Wylie C, Heasman J. 2001. Maternal VegT is the initiator of a molecular network specifying endoderm in *Xenopus laevis*. Development 128:167–180.

Yasuo H, Lemaire P. 1999. A two-step model for the fate determination of presumptive endodermal blastomeres in *Xenopus* embryos. Curr Biol 9:8869–8879.

Yew N, Oskarsson M, Daar I, Blair DG, Vande Woude GF. 1991. *mos* gene transforming efficiencies correlate with oocyte maturation and cytostatic factor activities. Mol Cell Biol 11:604–610.

Yoshizaki N, Soga M, Ito Y, Mao KM, Sultana F, Yonezawa S. 2004. Two-step consumption of yolk granules during the development of quail embryos. Dev Growth Differ 46:229–238.